Asian Journal of Scientific Research

ISSN 1992-1454

science alert
http://www.scialert.net

ANSInet
an open access publisher
http://ansinet.com

Asian Journal of Scientific Research 5 (4): 207-217, 2012
ISSN 1992-1454 / DOI: 10.3923/ajsr.2012.207.217

Effect of Calcination Temperature on the Transport Properties and Colloidal Stability of ZnO-water Nanofluids

K.S. Suganthi and K.S. Rajan
Centre for Nanotechnology and Advanced Biomaterials (CeNTAB), School of Chemical and Biotechnology, SASTRA University, Thanjavur-613401, India

Corresponding Author: K.S. Rajan, Seshasayee, Centre for Nanotechnology and Advanced Biomaterials (CeNTAB), School of Chemical and Biotechnology, SASTRA University, Thanjavur-613401, India Tel: 919790377951

ABSTRACT

Nanofluids are solid-liquid dispersions containing nanoparticles of size 1-100 nm in a liquid. Nanofluids that have enhanced thermal conductivity are best known for their application as coolants in food storage, transportation, refrigeration and air-conditioning industries. Considerable energy savings can be realized through the use of nanofluids as coolants. Viscosity is one of the major transport properties that determine the heat removal capability of nanofluids. The present study reports the effect of calcination temperature on the primary particle size, aggregate size of the ZnO nanoparticles and on the transport properties of the ZnO-water nanofluid. ZnO nanoparticles have been synthesized using Zinc nitrate hexahydrate as precursor. The primary particle size of the ZnO nanoparticles calcined at different temperatures ranging from 100-500°C was found to be in the range of 40-60 nm. The effect of calcination temperature on hydrodynamic size distribution of the ZnO nanoparticles has been investigated using dynamic light scattering technique. The viscosity of ZnO-water nanofluids, using ZnO powders prepared at different calcination temperatures have also been studied, along with their colloidal stability.

Key words: Nanofluids, calcination, aggregates, viscosity

INTRODUCTION

Nanofluids are dispersions containing nanoparticles having diameter of 1-100 nm. The term 'Nanofluid' was first coined by Choi (1995). The superior behavior of the solid-liquid dispersions compared to the liquid alone was first theoretically presented by Maxwell (1881). He theoretically proved that when solid particles were dispersed in a liquid, the resulting dispersion had higher thermal conductivity than the liquid. Since only micro or macro-sized particles were used for formulation of dispersions at that time, there was difficulty in attaining stable dispersions due to the rapid settlement of the particles. When they were used in heat transfer devices as coolants, erosion of the pipelines and clogging of channels were observed apart from increased pressure drop (Das *et al*., 2006). With the advent of nanotechnology, it became feasible to prepare dispersions of nanoparticles with enhanced transport properties which remained stable for months. When the nanoparticles replace the micro-or macro-sized particles, the aforesaid disadvantages can be overcome. Even with small amount of nanoparticles, a very high enhancement in thermal conductivity could be attained along with good colloidal stability, nominal rise in viscosity and a marginal increase in pressure drop (Das *et al*., 2006).

Nanofluids can be potentially used for a range of engineering applications. The primary application is the use of nanofluids as coolants for a wide array of devices ranging from electronic microchips (Wong and Leon, 2010) to nuclear reactors (Buongiorno *et al.*, 2008). With nanofluids as coolants, when higher heat transfer rates are achieved, the volume of the coolant used can be reduced considerably. Another important application of nanofluids is in enhancement of mass transfer. The nanoparticles in the dispersion increase the gas-liquid mass transfer by decreasing the resistance offered by the liquid film surrounding the gas bubble which is explained by grazing effect (Kars *et al.*, 1979). Oxygen transfer in bioreactors (Olle *et al.*, 2006; Olle and Wang, 2008), ammonia gas absorption in refrigeration systems (Kim *et al.*, 2006; Ma *et al.*, 2007), CO_2 absorption (Park *et al.*, 2006-2008) can be enhanced by using nanofluids. For the nanofluids to be efficiently used for these applications, the rise in viscosity should not be too high. A very large increase in viscosity will affect the heat transfer performance apart from the increased energy requirement for pumping. Hence, it becomes essential to investigate the rheology of the nanofluids.

There are a large number of investigations that have reported the transport properties of nanofluids. Masuda *et al.* (1993) reported enhanced thermal conductivity of dispersions containing ultra-fine particles of Al_2O_3, SiO_2 and TiO_2 even before the name 'Nanofluids' was coined. Though metal nanoparticles result in higher thermal conductivity of the nanofluids, metal oxides are the most exploited candidates for nanofluid preparation. This is due to the high flammability and rapid sedimentation of the metal nanoparticles due to their higher density (Kwak and Kim, 2005). Nanofluids formulated with metal oxides such as CuO (Namburu *et al.*, 2007; Gowda *et al.*, 2010), Al_2O_3 (Nguyen *et al.*, 2007; Zhu *et al.*, 2011), TiO_2 (Chen *et al.*, 2007; Turgut *et al.*, 2009) and Fe_2O_3 (Phuoc and Massoudi, 2009) have been widely investigated, whereas ZnO nanofluids (Lee *et al.*, 2010; Raykar and Singh, 2010) are not much exploited. This work focuses on the synthesis of ZnO nanoparticles, effect of calcination temperature on the properties of ZnO nanoparticles, formulation of ZnO-water nanofluids and investigation of the rheology and colloidal stability of the nanofluids.

MATERIALS AND METHODS

Materials: Zinc nitrate hexahydrate was purchased from Merck, India. Ammonium carbonate and methanol were purchased from Fisher Scientific, India and Loba Chemie, India, respectively. Sodium hexametaphosphate was procured from S D Fine-Chem Ltd., India. De-ionized water was used for the experiments.

Nanoparticle synthesis: ZnO nanoparticles were synthesized using precipitation method at room temperature (Chen *et al.*, 2008) using zinc nitrate hexahydrate as the precursor. Equimolar solution of ammonium carbonate was added to Zinc nitrate solution under continuous stirring to precipitate $Zn(OH)_2$ which was collected through filtration. The precipitate was washed several times with water and then with methanol. The precipitate was dried at 80°C for 5 h. The dried powder was calcined at different temperatures in the range of 100-500°C to convert $Zn(OH)_2$ to ZnO.

Nanofluid formulation: The nanofluid was formulated by two-step method in which nanoparticles were synthesized first and then dispersed in the liquid through either electrostatic stabihzation or steric stabilization. In this study, ZnO nanoparticles were dispersed using Sodium hexametaphosphate, as the dispersant at ZnO:Sodium hexametaphosphate ratio of 1:0.2. A predetermined quantity of ZnO powder was added to water with the dispersant under high shear

homogenization (IKA® T25, Ultra-Turrax®, Germany) for 20 min, followed by ultrasonication for 150 min (Vibra-cell™, Sonics, USA). The concentration of the nanofluid used in the study was 0.5% by volume.

Characterization of nanoparticles

Electron microscopy: Morphological characterization of as-synthesized and powder calcined at different temperatures was done using cold Field Emission Scanning Electron Microscope (JSM 6701F, JEOL, Japan). The sample was mounted on a brass stub using carbon tape and sputter coated with platinum and loaded into the specimen chamber. The samples were imaged at an acceleration voltage of 3 kV and at a working distance of 5.4 mm.

X-ray diffraction analysis: Crystalline nature of the as-synthesized and calcined powder was studied using X-ray diffractometer (X'PERT PRO, PANalytical, Netherlands). Cu-Kα-X-ray was used for the analysis. The temperature of measurement was 25°C. The X-ray scans were carried out between 2θ-values of 10 and 79.9° with a step size of 0.05°.

Spectroscopic analysis: Optical absorption spectra of the as-synthesized powder and those calcined at different temperatures were recorded in a UV-Visible spectrophotometer (Lambda 750, Perkin Elmer. Germany). The samples were scanned from 250 to 800 nm.

Thermal analysis: Thermal analysis of samples was done using SDT Q600, TA instruments, USA. About 2 mg of the sample was subjected to a controlled temperature rise from room temperature to 1000°C at the rate of 10°C min^{-1}.

Characterization of nanofluids

Hydrodynamic size distribution and colloidal stability: The hydrodynamic size distribution of the ZnO nanoparticles in the nanofluid was measured using a Zetasizer (Nano-ZS, Malvern Instruments, USA) which works on the principle of dynamic light scattering technique. Colloidal stability was ascertained by measuring the zeta potential of the ZnO-water nanofluids using the Zetasizer. For both measurement of hydrodynamic size and zeta potential, the nanofluid samples were diluted about 50 times with deionized water.

Viscosity: The Viscosity of nanofluids was measured using a viscometer (LVDV II+Pro, Brookfield Engineering, USA). The viscosity measurements were made at a shear rate of 73.4 s^{-1} using UL-adapter and spindle No. S00. Viscosities of the nanofluids were measured from room temperature to 55°C.

RESULTS

Characterization of nanoparticles

Morphology: Figure 1 and 2 show the influence of calcination temperature on the morphology of the samples at the magnification of 10000 and 50000, respectively. Figure 1a and 2a show the scanning electron micrographs of powders obtained without calcination (called as-synthesized samples). The as-synthesized ZnO nanoparticles (Fig. 1a, 2a) have irregular morphology and found to be in the form of aggregates. The samples calcined at 100°C (Fig. 1b, 2b) have a small fraction of particles with well defined spherical morphology, yet some large aggregates are present. As the calcination temperature was increased to 200°C (Fig. 1c, 2c), there was an increase in the

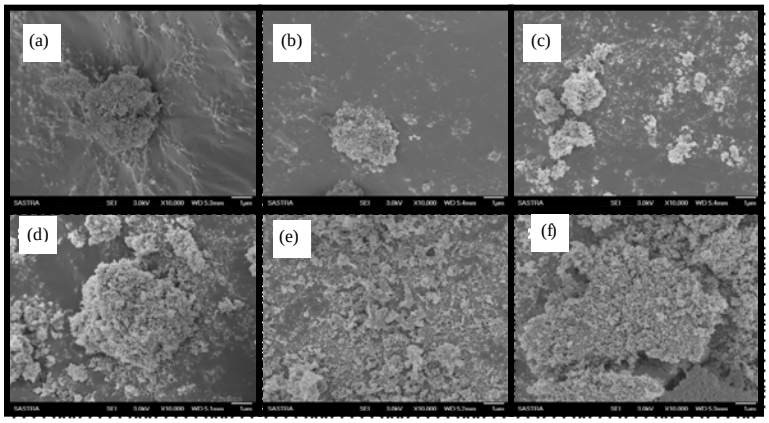

Fig. 1(a-f): Scanning electron micrographs of as-synthesized and powders calcined at different temperatures at a magnification of 10000

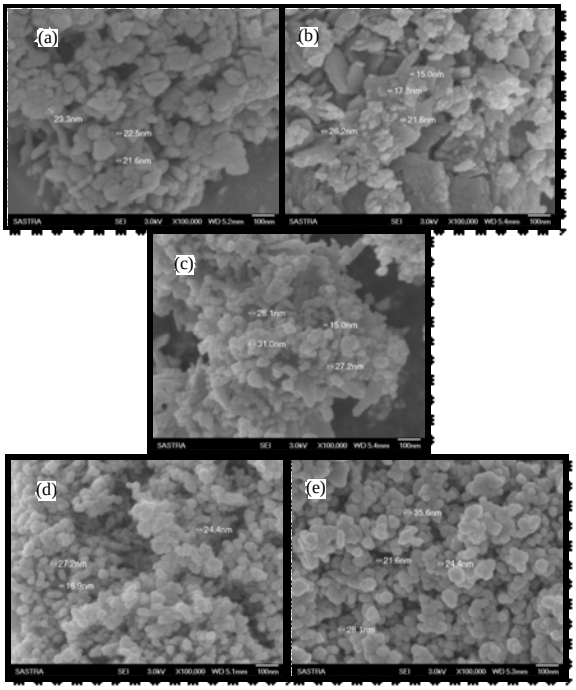

Fig. 2(a-e): Scanning electron micrographs of as-synthesized and powders calcined at different temperatures at a magnification of 50000

number of particles with well defined morphology. ZnO nanoparticles calcined at 300°C (Fig. 1d, 2d), 400°C (Fig. 2e) and 500°C (Fig. 1e, 2f) had well defined spherical morphology. There was no significant difference in the primary particle size between the ZnO nanoparticles calcined at different temperatures.

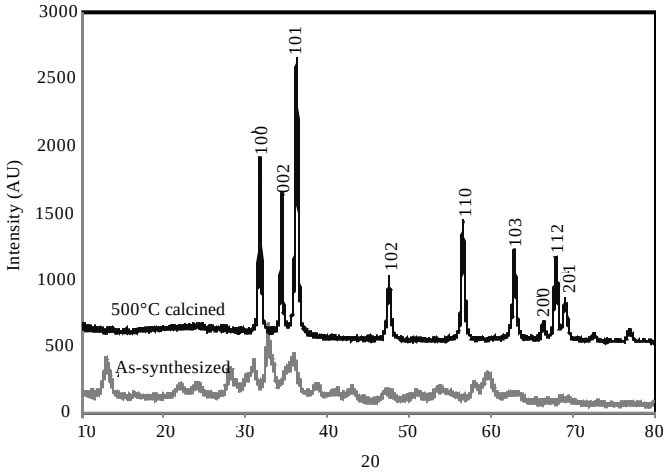

Fig. 3: X-ray diffraction spectra of as-synthesized nanoparticles and powder calcined at 500°C

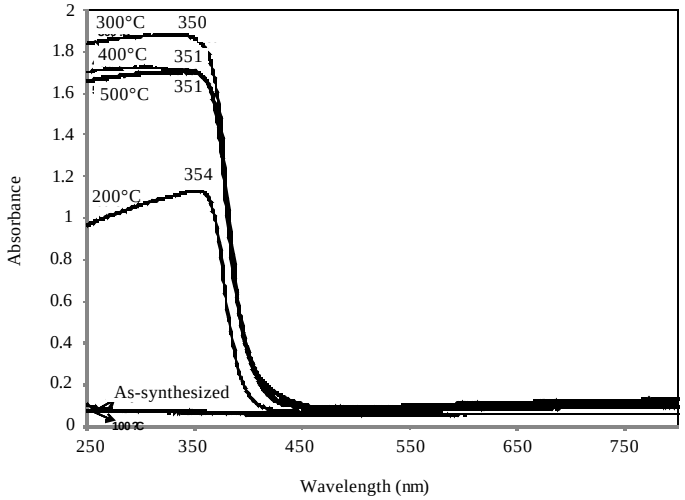

Fig. 4: UV-visible absorption spectra of as-synthesized powders and those calcined at different

Crystallinity: Figure 3 shows the X-ray diffraction patterns of as-synthesized and 500°C calcined ZnO nanoparticles. There were no distinct peaks in the XRD spectrum of the as-synthesized ZnO, highlighting the amorphous nature, whereas the well-defined peaks in the XRD spectrum of ZnO nanoparticles calcined at 500°C shows the high crystalline nature. The average size of the particles estimated using Scherrer equation were 21.79 and 24.23 nm, respectively for as-synthesized and 500°C calcined samples.

Spectroscopic analysis: The absorption spectra of assynthesized ZnO and ZnO calcined at different temperatures are shown in Fig. 4. The as-synthesized and 100°C calcined ZnO nanoparticles showed no specific peak between wavelengths 250 and 800 nm whereas ZnO nanoparticles calcined at 200, 300, 400 and 500°C showed peaks at 354, 350, 351 and 351 nm, respectively.

Thermal analysis: Figure 5 shows the change in weight of the ZnO nanoparticles subjected to the controlled temperature rise. The onset of a rapid decrease in weight was observed at 125°C (the decomposition temperature of $Zn(OH)_2$) which progressed upto 250°C. The percentage loss in weight from 125 to 250°C is 20.3%.

Characterization of nanofluids

Hydrodynamic size: Figure 6 shows the effect of calcination temperature on the average hydrodynamic size of particles in the prepared nanofluids. The nanofluid formulated with powder calcined at 100°C had the largest average aggregate size, 199.5 nm and that with powder calcined at 300°C had the smallest average aggregate size, 123.12 nm. A very small increase in average aggregate sizes was observed upon increasing the calcination temperature from 300 to 500°C.

Colloidal stability: Figure 7 shows the influence of calcination temperature on the zeta potential of the ZnO-water nanofluids. It is evident from Fig 7 that the absolute value of zeta potential increased as the calcination temperature was increased from 300 to 500°C.

Viscosity: Figure 8 shows the influence of calcination temperature on viscosity of ZnO-water nanofluids at 27.5 and 50°C. Nanofluid with 500°C calcined nanoparticles had the lowest viscosity both at 27.5 and 50°C.

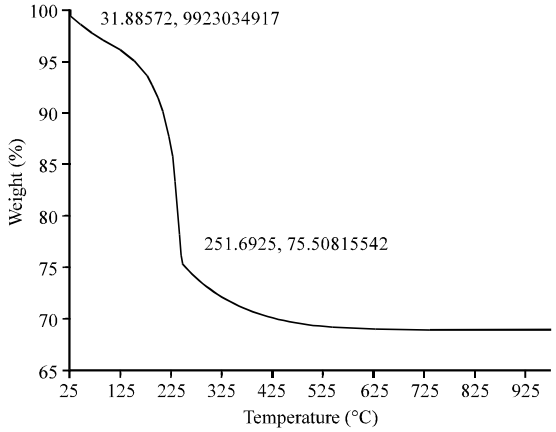

Fig. 5: Thermogram of as-synthesized powders

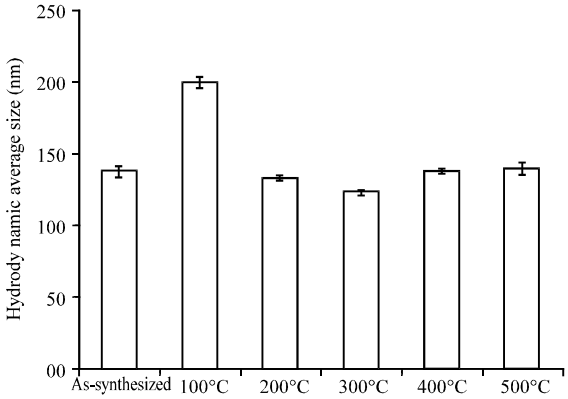

Fig. 6: Effect of calcination temperature on the average hydrodynamic size of ZnO nanoparticles

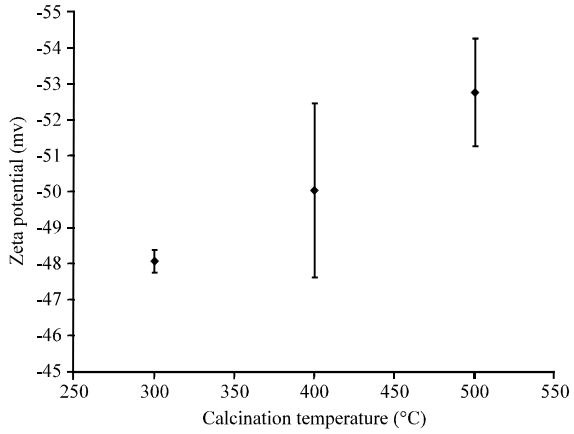

Fig. 7: Effect of calcination temperature on the Zeta potential of ZnO-water nanofluids

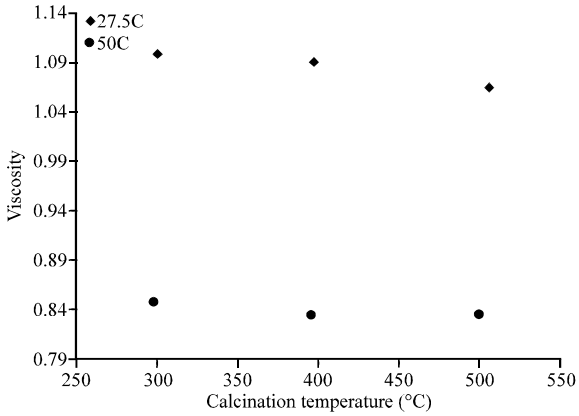

Fig. 8: Effect of calcination temperature on viscosity of ZnO-water nanofluids

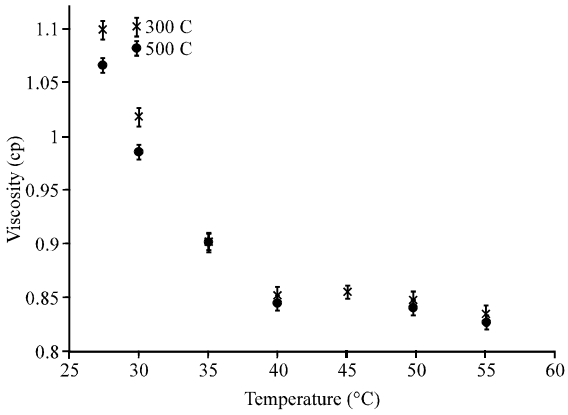

Fig. 9: Effect of temperature on viscosity of ZnO-water nanofluids formulated with ZnO nanoparticles calcined at different temperatures

Figure 9 shows the influence of temperature on viscosities of ZnO-water nanofluid formulated with ZnO nanoparticles calcined at 500°C, from which a non-linear decrease in viscosity with temperature is observed.

DISCUSSION

The decomposition temperature of $Zn(OH)_2$ is 125°C and hence the as-synthesized and 100°C calcined samples contain hydroxides only. The progressive increase in the fraction of the particles that have well defined spherical morphology and grain boundaries (Fig. 1, 2) for samples calcined at temperatures greater than or equal to 200 °C, is attributed to formation of ZnO particles from decomposition of $Zn(OH)_2$. This is also responsible for decrease in the fraction and the size of the aggregates with increase in calcination temperature.

The XRD spectrum of the calcined sample is in good agreement with XRD data reported by Moosavi *et al.* (2010), with the planes corresponding to the peaks shown in Fig. 3. The peaks confirm the presence of hexagonal phase of the wurtzite structure of ZnO. The role of calcination is of two folds: (1) conversion of $Zn(OH)_2$ to ZnO (2) phase transformation from amorphous to crystalline, as evident from Fig. 3, where the as-synthesized ZnO nanoparticles show amorphous character while the powder calcined at 500°C shows the characteristics of crystalline ZnO.

The electronic spectra (Fig. 4) of the calcined samples (calcination temperature = 200°C) are in good agreement with those reported by Chang and Tsai (2008). The absence of any characteristic absorption in the electronic spectra of as-synthesized sample and that calcined at 100°C also indicates that the decomposition of $Zn(OH)_2$ to ZnO has not occurred under those conditions.

During the decomposition of $Zn(OH)_2$, the theoretical mass reduction due to removal of H_2O is calculated to be 18.11% from stoichiometry. The experimental mass loss of 20.3% (Fig. 5) is close to this theoretical weight loss, confirming the decomposition of $Zn(OH)_2$ to ZnO. The difference between the calculated and experimental weight loss can be attributed to the free water molecules adsorbed on the surface of the nanoparticles.

The hydrodynamic size of the particles measured by dynamic light scattering technique assumes all the particles to be spherical in shape. When irregular shaped particles such as aggregates are present, the result might be misleading. Very large average size obtained for as-synthesized and 100°C calcined (Fig. 6) can be attributed to the presence of large aggregates as already shown in the scanning electron micrographs. Though the samples were ultrasonicated to break up the aggregates, the broken up aggregates with surfaces or part of the surfaces not stabilized by the surfactant molecules might have reagglomerated to form aggregates. Powders calcined above 300°C are more regular in size and shape and when dispersed with the aid of surfactant, are less prone to aggregation, resulting in smaller average size of those nanofluids.

Particle dispersions with absolute zeta potentials greater than 30 mV are considered as colloidally stable (Lee *et al.*, 2008). The absolute zeta potential values of the nanofluids with ZnO nanoparticles calcined at all temperatures are greater than 30 mV (Fig. 7) indicating that all the nanofluids are stable. This may be attributed to the increase in the number of particles with spherical morphology with increasing calcination temperature, as evident from the scanning electron micrographs (Fig. 1, 2). The role of surface area in several types of fluid-particle interactions involving interphase heat transfer has been well documented (Rajan *et al.*, 2006-2008). The finer nanoparticles possess more surface area enabling adsorption of surfactant molecules when compared to that of aggregates (lower exposed surface area) and hence the higher absolute zeta potential and colloidal stability of calcined powders.

Spherical nanoparticles offer less resistance to fluid flow than the non-spherical particles and hence the fluids containing spherical particles are less viscous than the fluids with non-spherical particles (Chen *et al.*, 2009). From the scanning electron micrographs, it was evident that nanoparticles calcined at 500°C have lesser fraction of aggregates (non-spherical) compared to the

powders calcined at other temperatures. This is responsible for lower viscosities observed with nanofluids prepared from powder calcined at 500°C (Fig. 8).

As the temperature of the nanofluid is increased, the particle-particle interactions and the intermolecular adhesion forces decrease resulting in the decrease in the viscosity of the nanofluid (Kole and Dey, 2011). The temperature dependence of nanofluid viscosity (Fig. 9) is similar to that of base fluid (water). The temperature reduction of nanofluid viscosity augers well for its use in cooling, as one could expect decreased viscosity during a heating cycle and hence improved heat extraction capability.

CONCLUSION

ZnO nanoparticles were synthesized by precipitation method using Zinc nitrate hexahydrate as precursor. ZnO nanoparticles are formed above decomposition temperature of $Zn(OH)_2$ (125°C), as evident from the spectroscopic analysis and thermal analysis. As the calcination temperature increased, regular spherical shaped ZnO particles formed with decrease in the fraction of aggregates and the crystalline nature of the powders increased. Powder calcined at 500°C was crystalline with wurtzite structure and spherical in morphology. Nanofluid formulated with 500°C calcined powder had the lowest viscosity and is more suitable for engineering applications. Nanofluids prepared with amorphous nanoparticles, when dispersed would have a larger fraction of aggregates and would be unstable due to particle settling. This leads to time-dependent viscosity which may decrease during shear due to de-agglomeration and re-agglomerate again in the absence of shear stress. Hence such nanofluids will be unreliable for real-time applications. Nanofluids prepared with crystalline nanoparticles and dispersed properly are less prone to aggregation and their viscosity will remain unaffected by time.

ACKNOWLEDGMENT

This study is supported by (1) INSPIRE fellowship (Reg.No.IF110312) of Department of Science and Technology (DST), India. (2) PG teaching grant No: SR/NM/PG-16/2007 of Nano Mission Council, Department of Science and Technology (DST), India (3) Grant No: SR/FT/ET-061/2008, DST, India and (4) Research and Modernization Project #1, SASTRA University, India. The authors thank SASTRA University for the infrastructural support extended during the work.

REFERENCES

Buongiorno, J., L.W. Hu, S.J. Kim, R. Hannink, B. Truong and E. Forrest, 2008. Nanofluids for enhanced economics and safety of nuclear reactors: An evaluation of the potential features, issues and research gaps. Nucl. Technol., 162: 80-91.

Chang, H. and M.H. Tsai, 2008. Synthesis and characterization of ZnO Nanoparticles having prism shape by a novel Gas condensation process. Rev. Adv. Mater. Sci., 18: 734-743.

Chen, H., Y. Ding and C. Tan, 2007. Rheological behaviour of nanofluids. New J. Phys., 9: 367-367.

Chen, C.C., P. Liu and C. Lu, 2008. Synthesis and characterization of nano-sized ZnO powders by direct precipitation method. Chem. Eng. J., 144: 509-513.

Chen, H., S. Witharana, Y. Jin, C. Kim and Y. Ding, 2009. Predicting thermal conductivity of liquid suspensions of nanoparticles (nanofluids) based on rheology. Particuology, 7: 151-157.

Choi, S.U.S., 1995. Enhancing Thermal Conductivity of Fluids with Nanoparticles. In: Developments and Applications of Non-Newtonian Flows, Siginer, D.A. and H.P. Wang (Eds.). American Society of Mechanical Engineers, New York, pp: 99-105.

Das, S.K., S.U.S. Choi and H.E. Patel, 2006. Heat transfer in nanofluids: A Review. Heat Transfer Eng., 27: 3-19.

Gowda, R., H. Sun, P. Wang, M. Charmchi, F. Gao, Z. Gu and B. Budhlall, 2010. Effects of particle surface charge, species, concentration and dispersion method on the thermal conductivity of nanofluids. Adv. Mech. Eng. 10.1155/2010/807610.

Kars, R.L., R.J. Best and A.A.H. Drinkenburg, 1979. The sorption of propane in slurries of active carbon in water. Chem. Eng. J., 17: 201-210.

Kim, J.K., J.Y. Jung and Y.T. Kang, 2006. The effect of nano-particles on the bubble absorption performance in a binary nanofluid. Int. J. Refrig., 29: 22-29.

Kole, M. and T.K. Dey, 2011. Effect of aggregation on the viscosity of copper oxide-gear oil nanofluids. Int. J. Therm. Sci., 50: 1741-1747.

Kwak, K. and C. Kim, 2005. Viscosity and thermal conductivity of copper oxide nanofluid dispersed in ethylene glycol. Korea-Aust Rheol. J., 17: 35-40.

Lee, J., P.E. Gharagozloo, B. Kolade, J.K. Eaton and K.E. Goodson, 2010. Nanofuid convection in microtubes. J. Heat Transfer. 10.1115/1.4001637.

Lee, J.H., K.S. Hwang, S.P. Jang, B.H. Lee, J.H. Kim, S.U.S. Choi and C.J. Choi, 2008. Effective viscosities and thermal conductivities of aqueous nanofluids containing low volume concentrations of Al2O3 nanoparticles. Int. J. Heat Mass Transfer, 51: 2651-2656.

Ma, X., F. Su, J. Chen and Y. Zhang, 2007. Heat and mass transfer enhancement of the bubble absorption for a binary nanofluid. J. Mech. Sci. Technol., 21: 1813-1818.

Masuda, H., A. Ebata, K. Teramae and N. Hishinuma, 1993. Alternation of thermal conductivity and viscosity of liquid by dispersing ultra-fine particles (dispersion of -Al2O3, SiO2 and TiO2 ultra-fine particles). Netsu Bussei (Japan), 4: 227-233.

Maxwell, J.C., 1881. A Treatise on Electricity and Magnetism. 2nd Edn., Clarendon Press, Oxford, UK..

Moosavi, M., E.K. Goharshadib and A. Youssefi, 2010. Fabrication, characterization, and measurement of some physicochemical properties of ZnO nanofluids. Int. J. Heat Fluid Flow, 31: 599-605.

Namburu, P.K., D.P. Kulkarni, D. Misra and D.K. Das, 2007. Viscosity of copper oxide nanoparticles dispersed in ethylene glycol and water mixture. Exp. Therm. Fluid. Sci., 32: 397-402.

Nguyen, C.T., F. Desgranges, G. Roy, N. Galanis, T. Mare, S. Boucher and H.A. Mintsa, 2007. Temperature and particle-size dependent viscosity data for water-based nanofluids-Hysteresis phenomenon. Int. J. Heat Fluid Flow, 28: 1492-1506.

Olle, B. and D.I.C. Wang, 2008. Novel and new concept to increase oxygen transfer in bioreactors. Chem. Eng. Trans., 14: 1-12.

Olle, B., S. Bucak, T.C. Holmes, L. Bromberg, T.A. Hatton and D.I.C. Wang, 2006. Enhancement of oxygen mass transfer using functionalized magnetic nanoparticles. Ind. Eng. Chem. Res., 45: 4355-4363.

Park, S.W., B.S. Choi and J.W. Lee, 2006. Effect of elasticity of aqueous colloidal silica solution on chemical absorption of carbon dioxide with 2-amino-2-methyl-1-propanol. Korea-Aust. Rheol. J., 18: 133-141.

Park, S.W., B.S. Choi, S.S. Kim and J.W. Lee, 2007. Chemical absorption of carbon dioxide into aqueous colloidal silica solution containing monoethanolamine. J. Ind. Eng. Chem., 13: 133-142.

Park, S.W., B.S. Choi, S.S. Kim and J.W. Lee, 2008. Mass transfer of carbon dioxide in aqueous colloidal silica solution containing N-Methyldiethanolamine. Korean J. Chem. Eng., 25: 819-824.

Phuoc, T.X. and M. Massoudi, 2009. Experimental observations of the effects of shear rates and particle concentration on the viscosity of Fe2O3-deionized water nanofluids. Int. J. Therm. Sci., 48: 1294-1301.

Rajan, K.S., S.N. Srivastava, B. Pitchumani and B. Mohanty, 2006. Simulation of gas-solid heat transfer during pneumatic conveying: Use of multiple gas inlets along the duct. Int. Commun. Heat Mass, 33: 1234-1242.

Rajan, K.S., B. Pitchumani, S.N. Srivastava and B. Mohanty, 2007. Two-dimensional simulation of gas-solid heat transfer in pneumatic conveying. Int. J. Heat Mass Trans., 50: 967-976.

Rajan, K.S., K. Dhasandhan, S.N. Srivastava and B. Pitchumani, 2008. Studies on gas-solid heat transfer during pneumatic conveying. Int. J. Heat Mass Trans., 51: 2801-2813.

Raykar, V.S. and A.K. Singh, 2010. Thermal and rheological behavior of acetylacetone stabilized ZnO nanofluids. Thermochim. Acta, 502: 60-65.

Turgut, A., I. Tavman, M. Chirtoc, H.P. Schuchmann, C. Sauter and S. Tavman, 2009. Thermal conductivity and viscosity measurements of water-based TiO_2 nanofluids. Int. J. Thermophys., 30: 1213-1226.

Wong, K.V. and O.D. Leon, 2010. Applications of Nanofluids: Current and future. Adv. Mech. Eng. 10.1155/2010/519659

Zhu, H., D. Han, Z. Meng, D. Wu and C. Zhang, 2011. Preparation and thermal conductivity of CuO nanofluid via a wet chemical method. Nanoscale Res. Lett., Vol. 6, 10.1186/1556-276X-6-181